



Correlation analysis of agricultural drought risk on wet farming crop and meteorological drought index in the tropical-humid region

Amalia Nafisah Rahmani Irawan¹ · Daisuke Komori^{1,2} · Vempi Satriya Adi Hendrawan³

Received: 10 May 2022 / Accepted: 11 April 2023 / Published online: 28 April 2023
© The Author(s) 2023

Abstract

In the tropical-humid region, wet farming crops (e.g., paddy) are a common agricultural commodity with a high-water requirement. Usually planted in the Asia monsoon region with a high precipitation rate, these crops are divided into the wet cropping season and the dry cropping season. During the dry cropping season, they are particularly vulnerable to agricultural drought caused by the decrease in precipitation. This study used Indonesia as a case study and is aimed at assessing the agricultural drought risk on a wet farming crop during the dry cropping season by examining the correlation between the drought hazard and its risk. For hazard assessment, Standardized Precipitation Index (SPI) was used to assess the agricultural drought, by using the Global Satellite Mapping of Precipitation (GSMaP) which has $0.1^\circ \times 0.1^\circ$ spatial resolution. The result of correlation analysis between the SPI and drought-affected areas on a city scale showed that SPI-3 in August is the most suitable timescale to assess the agricultural drought in Indonesia. The agricultural drought risk assessment was conducted on the grid scale, where the crop yield estimation model was developed with the help of Normalized Difference Vegetation Index (NDVI). Based on the correlation analysis between SPI-3 and the detrended crop yield as drought risk indicators, the higher yield loss was found in the area above the threshold value (r -value ≤ 0.6) indicating that those areas were more vulnerable to drought, while the area below the threshold value has lower crop yield loss even in the area that was hit by the most severe drought, because the existing irrigation system was able to resist the drought's impact on crop yield loss.

1 Introduction

The Intergovernmental Panel on Climate Change (IPCC) reported 2018 that the global temperature is expected to increase by 1.5°C by 2030. This warming trend, as noted by the National Center for Atmospheric Research (NCAR), will result in unevenly distributed changes in evaporation and precipitation rate, potentially leading to more frequent and severe floods in some areas and droughts in others (Lehner et al. 2006; Trenberth 2005; Hirabayashi et al. 2008). Drought is one of the extreme climate events, and referring to Wilhite and Glantz (1985), there are four types of droughts, starting with meteorological droughts or when an

area experiences a water deficiency compared to its normal condition. Over time, this lack of precipitation could lead to an agricultural drought or when there is depletion of soil moisture (Legesse 2010) that could cause impaired growth and crop yield reduction. If the deficiency of precipitation is still going, it can cause a low water supply on the surface (e.g., river, lake) and groundwater. And for the socioeconomic, drought occurs when there is a decrease in supply and an increase in demand for water that can affect the social, economic, and environmental conditions.

According to the Food and Agriculture Association (FAO), drought affected agriculture areas the most, absorbing around 80% of direct impacts with multiple effects on agricultural production, food security, and rural livelihoods, especially in the developing countries. For the drought assessment study, a variety of drought indexes have been developed based on precipitation or well known as the meteorological drought index. One of such indexes is the Standardized Precipitation Index (SPI), which was founded by McKee et al. 1993, and can be used to assess drought using long-term precipitation data (minimum 20–30 years). The SPI uses probability density functions and normalization

✉ Amalia Nafisah Rahmani Irawan
amalia.nafisah.rahmani.irawan.q3@dc.tohoku.ac.jp

¹ Graduate School of Environmental Studies, Tohoku University, 980-8572 Sendai, Japan

² Green Goals Initiative, Tohoku University, Sendai 980-8577, Japan

³ Department of Civil and Environmental Engineering, Universitas Gadjah Mada, 55284, Yogyakarta, Indonesia

to assess the wet and dry conditions in a given region. A description of the calculation of SPI can be found in the works of McKee et al. (1993), Angelidis et al. (2012), and many other literatures. Related with the determination of the probability density function (refer to the original document by McKee et al. (1993)), the two-parameter gamma distribution is utilized to fit the cumulative precipitation data while there is still ongoing debate within the literature about which distribution function is more suitable to use (Pieper et al. 2020). Beside a simple gamma distribution which was used directly by many researchers on their drought assessment using SPI (Karavitis et al. 2011; Shah et al. 2015; Pramudya and Onishi 2018; Hendrawan et al. 2022), the Pearson type III distribution which was suggested by Guttman (1999) as the more appropriate to describe observed precipitation is also often used directly in the calculation algorithm for the SPI (Blain. 2011; Naresh et al. 2012; Ribeiro and Pires 2016; Ionita et al. 2021). Additionally, researchers have studied the influence of different probability distributions on the results of the SPI, as well as identifying the most suitable probability density function for their particular study (Angelidis et al. 2012; Stagge et al. 2015; Wang et al. 2019; Pieper et al. 2020; Shiau 2020; Ying and Li 2020; Moccia et al. 2022).

In this research, the category of SPI condition is referred to the threshold set by the World Meteorological Organization (WMO) user guidelines, as shown in Table 1. Basically, the dry condition is identified when the SPI value is less than or equal to negative one ($SPI \leq -1$). One advantage of the SPI is its versatility in terms of timescales, as it can be calculated for various periods of interest (ranging from 1 month to multiple months) according to the user's interest (WMO 2012) and using any month as a reference (from January to December). For example, the SPI-3 index is based on the cumulative precipitation over a 3-month period, with the reference month determining the specific months that are used in the calculation. If the reference month is August, the SPI-3 index would be based on the cumulative precipitation during June, July, and August.

Although the SPI was originally recommended to assess meteorological drought, numerous research studies have also used it to assess agricultural drought. For example, Geng et al. (2016) assessed the agricultural drought hazard on a global

scale from 1980 to 2008. Umran in 1999 found that in Turkey, SPI-3 is sensitive to soil moisture, implying that there is a reduction in soil moisture that affects crop growth. But even though many studies have been conducted based on SPI, there is no general agreement reached to determine the most appropriate timescale for agricultural drought assessment. For example, in 2021, Kumar et al. found that SPI-1 has a strong correlation with the percentage of departure, a simple drought index that defined a percentage of precipitation deviation from normal condition. Additionally, in 2003, Ji and Peters stated that SPI-3 has a good correlation with the Normalized Difference Vegetation Index (NDVI), one of the vegetation indices in the U.S. Great Plains. Dutta et al. 2013, said that SPI-3 is a good indicator of anomalies for grain yields in the arid and semi-arid regions in India. Meanwhile Dai et al. 2020, found that the 4 months of SPI scale is suitable in monitoring agricultural drought in the Pearl River Basin. And Iglesias and Quiroga 2007 used SPI-12 as a climate indicator for measuring the climatic risk to cereal production. But there is still less discussion on agricultural drought assessment on the wet farming crop.

According to FAO, the wet farming crop (e.g., paddy) is a common agriculture commodity in the tropical-humid region that needs a relatively large amount of water (450–700 mm/total growing period). This region is defined by a mean monthly temperature exceeding 18 °C, rainfall exceeding evapotranspiration for at least 270 days in a year, and usually irrigated cropland (Salati and Vose (1983), Lugo and Brown 1992). In the tropical-humid region, wet farming crops have two primary planting periods: the wet planting period during the rainy season and the dry planting period during the dry season. The crop productivity is relatively higher during the dry cropping period as there is more sunlight available to support crop growth only if there is a sustained water supply.

In addition, to understand the risk of drought in agriculture, many studies also used vegetation indices obtained from satellite datasets. According to Xue and Su (2017), vegetation indices often rely on remote sensing over vegetation canopies to evaluate and quantify vegetation cover, vigor, and growth dynamics, as well as provide qualitative assessments. There are many kinds of vegetation indices; one of them is the NDVI, often used to quantify biomass or vegetation by measuring the difference between near-infrared light (which vegetation strongly reflects) and red light (which vegetation absorbs). The values of the NDVI vary from -1 that is highly likely water to $+1$, which means dense green vegetation. Besides monitoring vegetation conditions, many researchers have used NDVI for crop yield estimation; for example, Maselli and Rembold (2001) in the Mediterranean African countries used monthly global area coverage (GAC) NDVI, Mkhabela et al. (2005) generated corn yield estimation in Swaziland using decadal average NDVI data, Balaghi et al. (2008) used NDVI to predict wheat in Morocco, and Son et al. (2014) used NDVI to generate estimation for rice in South Vietnam.

Table 1 The category of SPI values

2.0+	Extremely wet
1.5 to 1.99	Very wet
1.0 to 1.49	Moderately wet
– 0.99 to 0.99	Near normal
– 1.0 to – 1.49	Moderately dry
– 1.5 to – 1.99	Severely dry
– 2 and less	Extremely dry

This study was aimed at addressing the gap in agricultural drought discussions concerning wet farming crops, particularly in the tropical-humid region. This research was conducted to assess the agricultural drought on wet farming crops during the dry cropping season with objectives as follows: (i) to identify the most suitable SPI for agricultural drought assessment in the tropical-humid region and (ii) to examine the spatial response of the wet farming crop during the dry cropping season to agricultural drought on a grid scale. The study findings will provide insight into the effect of agricultural drought on wet farming crops.

2 Study location

Indonesia is a major producer of agricultural products (FAO 2003), with 31.46% of its land being agricultural land (World Bank, 2016). This study was conducted in one of the provinces in Indonesia, West Java, which refers to its Planning Board's official website and is located between 5° 50'–7° 50' south latitude and 104° 48'–108° 48' east longitude with the mountainous area encompassing the middle and south area, while the lowland is in the north area. The province is in the tropical-humid region and experiences a monsoon climate with annual precipitation ranging from 2000 to 4000 mm. West Java has a wet season from October to March and a dry season from April to September. Figure A.1 in the Appendix shows the precipitation distribution in West Java, and during the dry season, the average precipitation is around 100–150 mm, while the lowest precipitation occurred in August with less than 50 mm. Maryati et al. (2018) reported that 50.2% of West Java's total area (35,377,76 km²)

is agricultural land, mainly comprising paddy fields. With the supportive weather condition, the farming activity is intensive, with double to triple crop rotations per year, and it contributes approximately 17.8% to the national rice stock.

Figure 1 shows the location of the agricultural area in West Java. The agriculture areas are very dispersed but mainly concentrated in the northern part. The study area is shown in green color, while the red color represents the agriculture area that was excluded from this study because it was an expansion in 2018 located in Banjar and Pangandaran Regency. Meanwhile, the orange color indicated the agriculture area located in Bogor Regency, which is not included in this study because the preliminary analysis resulted in a low correlation between observed precipitation data and satellite-based precipitation data used in this research. As for the historical drought event, Surmaini and Faqih (2016) compared the impact of climate extreme on paddy fields in Indonesia from 1999 to 2015 and found that drought affected a larger area of paddy fields than floods. They also reported that during the El Niño event, the dry cropping season was affected by a lack of water supply, leading to an increased change of crop failure. D'Arrigo and Wilson (2008) found that during El Niño in 1997/1998, paddy production in Java alone decreased by up to three million tons compared to the previous year.

3 Materials and method

3.1 Study framework

The flowchart in Fig. 2 outlines the two main parts of this research, represented in blue and green colors. The blue

Fig. 1 The map of agriculture area in West Java, Indonesia

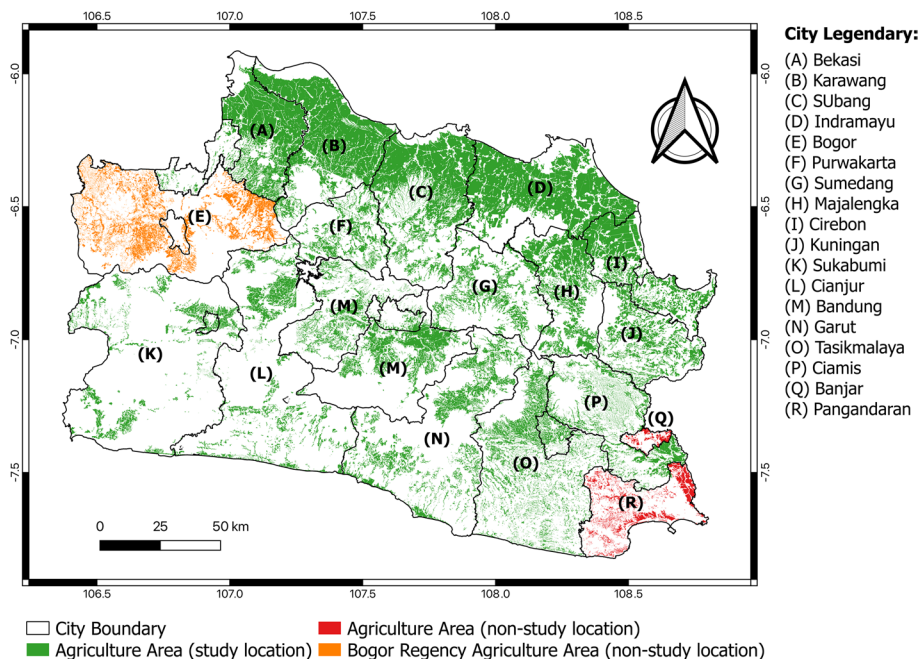
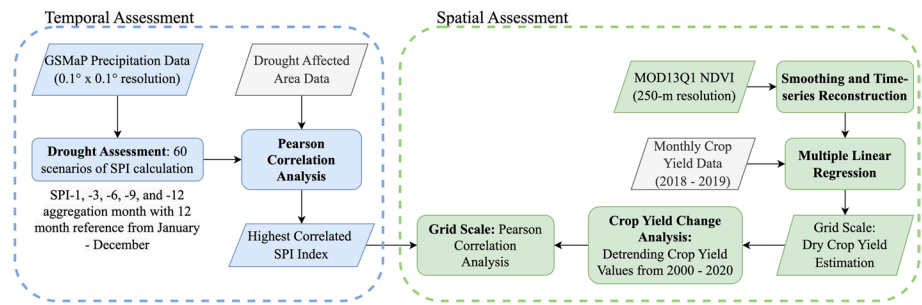


Fig. 2 Research framework



section focuses on temporal assessment, which begins with drought assessment using SPI. SPI was calculated for 60 scenarios from various SPI aggregation timescales (SPI-1, SPI-3, SPI-6, SPI-9, and SPI-12) and various month references from January until December. Then, the correlation analysis was assessed between the SPI and drought-affected areas (Dai et al. 2020) to determine the most suitable SPI which has the highest correlation. The green section is dedicated to spatial assessment, where the dry crop yield on a grid scale was estimated using multiple linear regression method between the NDVI and subround crop yield data during the dry cropping season. Finally, the correlation between the selected SPI and detrended crop yield value is analyzed to assess the spatial response of the wet farming crop during the dry cropping season to agricultural drought.

3.2 Materials

3.2.1 Precipitation data

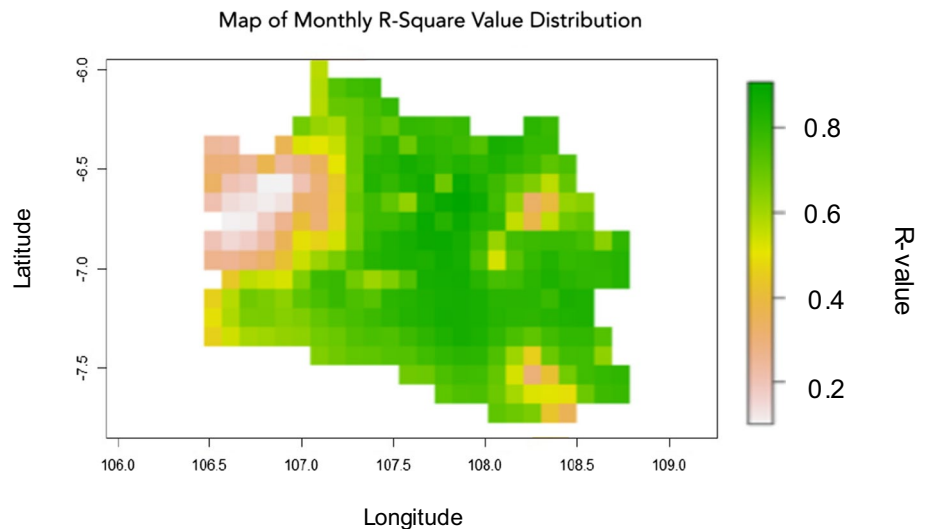
The precipitation data were obtained from the Global Satellite Mapping of Precipitation (GSMaP), a near real-time rainfall data provided by the Japan Aerospace Exploration Agency (JAXA), and retrieved from the following link:

<https://sharaku.eorc.jaxa.jp/GSMaP/>. The daily precipitation data, covering the period from April 2000 to March 2021, were retrieved across West Java with a resolution of $0.1^\circ \times 0.1^\circ$. Prior to using the GSMaP data for SPI calculation, a preliminary analysis was conducted to examine the agreement between the observed precipitation data and satellite-based precipitation data (Mourtzinis et al. 2017).

This preliminary analysis utilized observed precipitation data from the Meteorology, Climatology, and Geophysical Agency in Indonesia spanning from January 1981 to March 2013. There were 52 stations across 16 regencies with average area coverage reaching 680.38 km² per station. Since the observed precipitation data were provided on a point scale, the inverse distance weighted (IDW) method was applied to estimate the precipitation in unmeasured locations and to produce the precipitation distribution in West Java. Meanwhile, for the satellite-based precipitation data, the GSMaP data was used, which is available from March 2000 to the present date. Finally, the coefficient of determination or *R*-square (*R*²) was examined by using the precipitation data within the available period from both datasets spanning from April 2000 to March 2013.

The distribution of *R*-square value result is shown in Fig. 3, where the greenish color indicated a high agreement

Fig. 3 Map of monthly *R*-square value distribution in West Java



while the reddish color indicated a low agreement between the GSMaP and observed precipitation data. Tashima et al. (2020) noted that the GSMaP dataset frequently underestimates precipitation data and it was caused by the location of Indonesia that is located in the equator where land and sea coexist, which can lead to greater relative error in GSMaP observations. However, they also mentioned that this condition is not a problem for drought assessment because the distribution was normalized during SPI calculation. But in this research, the area with a low agreement (R -square < 0.5) was excluded to avoid uncertainty in the drought assessment process due to insufficient data accuracy.

3.2.2 Agricultural statistical dataset

As previously mentioned, West Java has two cropping seasons: the wet cropping season from October to March and the dry cropping season from April to September. The Ministry of Agriculture provided data on the agricultural areas affected by drought during the dry cropping season, while the Statistical Bureau of West Java provided annual data on crop production and harvested area from 2000 to 2021, without separating the data by cropping season. Additionally, the monthly dataset of crop production and crop harvested area is available for a limited time or from 2018 to 2019 and was used to generate the grid-scale crop yield estimation model. In this study, the crop yield was calculated using the equation below:

$$\text{CropYield} \left(\frac{\text{Ton}}{\text{Ha}} \right) = \frac{\text{CropProduction}(\text{Ton})}{\text{HarvestedArea}(\text{Ha})} \quad (1)$$

3.2.3 Vegetation index data

Normalized Difference Vegetation Index analysis was conducted to quantify vegetation biomass by measuring the difference between near-infrared light (NIR), which vegetation strongly reflects, and red light, which vegetation absorbs. The values vary from -1 that is highly likely water; 0 , which means an urban area; and $+1$, which means dense green vegetation. NDVI value was calculated following this equation:

$$\text{NDVI} = \frac{(\text{NIR} - \text{RedLight})}{(\text{NIR} + \text{RedLight})} \quad (2)$$

In this study, the NDVI was retrieved from Moderate Resolution Imaging Spectroradiometer or MODIS-Terra (MOD13Q1) version 6. The data were downloaded from <https://lpdaac.usgs.gov/products/mod13q1v006/> specifically the h28v09 tile, which covers the West Java area. The dataset has a 250-m resolution and 16-day interval, with 23 images available annually from March 2001 to the present. The

details of each image and the retrieval date for each cropping season can be seen in Table 2. Although the study focuses on the wet farming crops during the dry cropping season, the complete images were needed for the NDVI time-series reconstruction process; thus, the wet farming cropping season was included at the beginning.

3.3 Method

3.3.1 Drought assessment

Drought assessment was conducted using the SPI as one of the meteorological-based indices using the GSMaP precipitation dataset. SPI was founded by McKee et al. 1993 and recommended by WMO as an indicator of wet and dry conditions in certain regions. The SPI value is calculated basically by using long-term precipitation data and fitted to a probability distribution, which is then transformed into a normal distribution such that the mean SPI is zero for a specific location and desired period. However, the determination of an appropriate probability density function to be utilized is beyond the scope of this study. Therefore, adhering to the original research by McKee et al. (1993) and the recommendation from WMO, this study used the gamma distribution to obtain the SPI value. For the result, positive SPI values indicate above-average precipitation, whereas negative values indicate below-average precipitation.

In SPI analysis, the aggregation timescale can be adjusted based on the user's interest. For example, to evaluate short-term drought conditions, SPI-1 or SPI-3 can be used, which utilize the cumulative rainfall for 1 month

Table 2 The details of NDVI image retrieval date

Cropping season	Detail of NDVI images and retrieval dates	
Dry cropping season	NDVI-7: 7 April	NDVI-13: 12 July
	NDVI-8: 23 April	NDVI-14: 28 July
	NDVI-9: 9 May	NDVI-15: 13 August
	NDVI-10: 25 May	NDVI-16: 29 August
	NDVI-11: 10 June	NDVI-17: 14 September
	NDVI-12: 26 June	NDVI-18: 30 September
Wet cropping season	NDVI-19: 16 October	NDVI-1: 1 January
	NDVI-20: 1 November	NDVI-2: 17 January
	NDVI-21: 17 November	NDVI-3: 2 February
	NDVI-22: 3 December	NDVI-4: 18 February
	NDVI-23: 19 December	NDVI-5: 6 March
		NDVI-6: 22 March

and 3 months respectively. The procedures for calculating SPI can be found in several references, such as McKee et al. (1993), Guttman (1999), Vicente-Serrano and López-Moreno (2005), and the WMO user guidelines (2012).

Because this study is conducted to assess the agricultural drought on the wet farming crop, the SPI analysis will be limited on agricultural areas in West Java. Furthermore, the first objective of this study is to determine the most correlated SPI aggregation timescale to assess agricultural drought on the wet farming crop. To achieve this, the SPI will be calculated for various aggregation timescales: SPI-1, SPI-3, SPI-6, SPI-9, and SPI-12, with various month references from January to December, resulting in a total of 60 SPI. These indices will be correlated with NDVI and agriculture statistical datasets. Then, the SPI will be interpolated using a linear method to the same resolution as NDVI or 250-m resolutions. The interpolated SPI will be used for spatial analysis on a grid scale.

3.3.2 Crop yield model

The NDVI time-series reconstruction was used to generate the crop yield estimation model (Huang et al. 2014) on the grid scale. This process was limited to the agricultural areas in West Java, so the dataset was masked by the agriculture area shapefile obtained from Indonesia's Geospatial Information Agency. Prior to analysis, the images underwent pre-processing to remove the unfavorable atmospheric condition (Pan et al. 2015). This included image mosaicking to ensure the study location coverage, layer stacking of all the NDVI images to construct a time series, and smoothing of the NDVI time series. For the smoothing, the Savitzky-Golay filtering was applied to the NDVI time series (Chen et al. 2004) from 2001 to 2021. Then, to eliminate non-significant variables, the stepwise multiple linear regression model was used (Freund and Litell 1991), generating a crop yield model on each grid following this equation:

$$Y = \alpha + \beta_1 X_1 + \beta_2 X_2 + \dots + \beta_i X_i \quad (3)$$

where Y is dry season crop yield (ton/Ha), α intercept, β_i slope for X_i , and X_i smoothed NDVI (dry cropping season).

Due to the limited data availability, which were only available from 2018 to 2019 among 15 regencies, the dataset was divided into 70% training data for model development based on the above equation and 30% for model validation. The crop yield estimation model was constructed using NDVI as the predictor variable and crop productivity data during the dry cropping season, which means it will only include the NDVI-7 until NDVI-18 into consideration.

Once the model is validated, it will be used to predict the dry season crop yield values at the grid level from 2000 to 2020.

3.3.3 Temporal and spatial scale analysis

The temporal analysis was intended to determine the most suitable aggregation timescale for drought assessment in West Java. This goal was achieved by assessing the Pearson correlation between the SPI obtained from the drought assessment process and the drought-affected areas. Because this research was limited to the dry cropping season, the SPI were selected from the dry season precipitation only. Finally, the SPI with the highest correlation was chosen as the most suitable.

For the spatial analysis, it was conducted to examine the response of the wet farming crop during the dry cropping season to agricultural drought in each region on the grid scale. The response was determined by examine the decrease of crop yield, as agricultural drought risk indicator, during the drought period which is indicated by the SPI. Thus, this objective was achieved by assessing the correlation between the SPI and the agricultural drought risk indicator. Because of the characteristic of the agricultural area in West Java, which is very fragmented, a finer resolution was needed to examine the response on a local scale. To match the resolution of the crop yield model on a grid scale, using linear interpolation, the distribution of SPI around West Java was downscaled from $0.1^\circ \times 0.1^\circ$ resolution to 250-m resolution.

Prior to conducting the correlation analysis, the LOWESS (locally weighted scatterplot smoothing) technique was used to eliminate the influence of technological advancements on crop yield trends. Then, the detrended crop yield was determined by dividing the actual crop yield by the trend. The result of this detrended method varies around 1, which means that crop yield with a value of 1 is indicated as the normal condition, crop yield value larger than one is indicated as crop yield gain, and crop yield value lower than one is indicated as crop yield loss. Then, the Pearson correlation analysis was performed between the drought event (indicated by $SPI \leq -1$) and detrended crop yield values on the grid scale. To ensure the impact of drought on crop yield was correctly examined, the most severe drought year was selected as a target period for assessing the spatial response of wet farming crops during the dry cropping season. Additionally, only significant grids were included in the spatial response assessment.

Finally, the map of distribution will be generated to examine the response of the wet farming crops to agricultural drought during the dry cropping season at each grid. Additionally, the grid scale will be categorized based on the presence of an irrigation system served by the dam obtained

from Sianturi et al. (2018) and the information provided by the Government of Indonesia. This process was conducted to examine the different responses between the agriculture area served by a dam (will be referred to as dam-irrigated areas) and the agriculture area where water supply is obtained from rivers and wells (will be referred to as local water resource-irrigated areas) to drought.

4 Result and discussion

4.1 Temporal assessment

The temporal assessment was started with a drought assessment using SPI. As previously mentioned on the methodology section, there were a total of 60 scenarios of SPI calculated consisting of different SPI aggregation timescales: SPI-1, SPI-3, SPI-6, SPI-9, and SPI-12 based on the month reference in January, February, March, April, May, June, July, August, September, October, November, and December. This calculation used the monthly GSMaP dataset from 2000 to 2020 with $0.1^\circ \times 0.1^\circ$ resolution. Appendix 1 shows the monthly variability of precipitation distribution from January to December across West Java. And to obtain the target area, the result was masked with an agriculture area shapefile. For the temporal assessment, which was conducted on city-scale analysis, the SPI on each regency was calculated using the average value of contributing grid cells.

After all 60 scenarios of the SPI on the city scale were calculated, the correlation analysis was assessed to determine the most suitable SPI aggregation timescale to be utilized for agricultural drought assessment in West Java. For this analysis, the drought-affected area data was used as an agricultural drought risk indicator. This data was obtained from 2000 to 2018 on a city scale. Even though this data was limited in terms of spatial resolution, it was deemed suitable for characterizing agricultural drought risk as it was provided by the Ministry of Agriculture and represents the affected areas by drought during the dry cropping season. The Pearson correlation analysis was calculated separately between drought-affected areas and the SPI in 15 regencies.

The outcome of this process was the r -value in each of the 60 scenarios on a city level, with detailed results provided in the form of a table included in the Appendix. In order to help with the interpretation of the correlation result, Fig. 4 shows the heatmap of the average correlation value. The vertical axis indicated the SPI aggregation timescale and the horizontal axis indicated the month reference. Please note that the black color in the heatmap involved only a wet season, which is not a target period of this study, so the result was excluded.

The heatmap analysis indicates that all scenarios of the SPI produced negative correlations, represented by the red color. This result can be interpreted that the decrease in SPI, or a dry condition, is associated with an increase of drought-affected areas in the agricultural region. In addition, the highest negative correlation was produced during the SPI-3 in August (r -value = -0.59 and p -value < 0.05). Thus, it can be concluded that this index can be used to examine the impact of agricultural drought because in all the regencies, the drought condition that was represented by this index was corresponding with the drought-affected areas. Moreover, the index's timescale coincides with the peak of the dry season, which is very significant to crop production during the dry cropping period.

Additionally, the result shown here is consistent with Umran's study in 1999, which stated that SPI-3 is sensitive to the reduction in soil moisture that affects crop growth. This outcome suggested that to assess the response of the wet farming crop to drought in West Java, SPI-3 in August is the most suitable SPI. However, as the limitation on this analysis, we only considered the temporal and spatial scale as drought's dimensions without separating the impact that might be caused by other dimension such as drought intensity and timing. Following the temporal analysis, the spatial analysis was conducted by using the value of SPI-3 index in August for the correlation analysis with detrended crop yield on the grid scale. Even though the spatial analysis was conducted on the grid scale while the temporal analysis result was obtained on the city-scale assessment, the difference in spatial resolution is not much of a problem because the SPI was calculated based on the rainfall data, which cover relatively large area. The assumption is that the deficiency

Fig. 4 Heatmap of mean of correlation value between SPI and drought-affected areas.

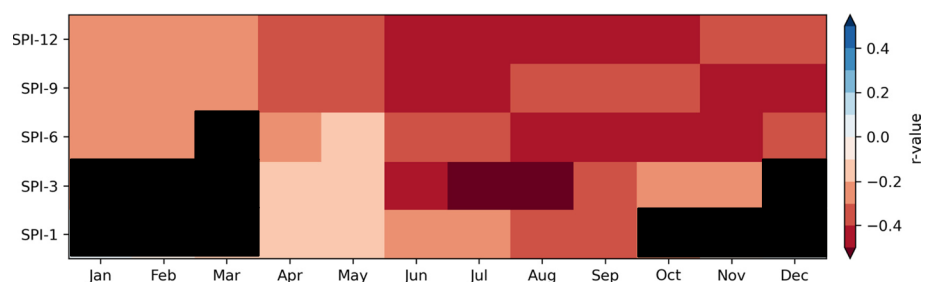
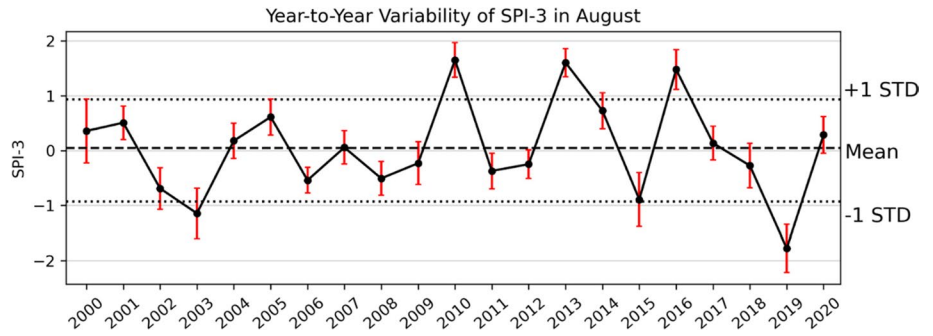


Fig. 5 Year-to-year variability of SPI-3 in August



of rainfall that can trigger drought events can be observed on a large-scale resolution, and it is also reflected on the smaller scale one.

Additionally, as mentioned in the methodology section, the most severe drought year was selected as the focus period for spatial scale assessment. Figure 5 shows the variability of the SPI throughout the year across all areas in West Java. The vertical axis indicated the SPI while the horizontal axis indicated the year from 2000 to 2020 as the study period. The result showed that year 2019 has the lowest SPI, which can be understood as the most severe drought year in West Java, which is thus used as the focus period for spatial scale assessment.

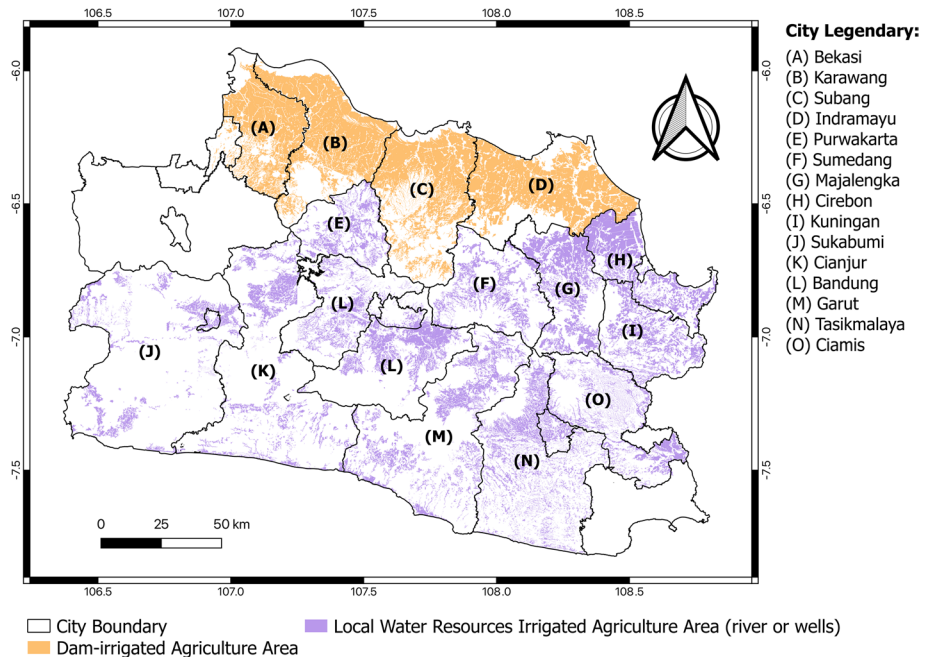
Additionally, in terms of agricultural practices especially for wet farming crops, one of the key factors is the delivery system of water supply to the paddy fields or irrigation systems. As a preliminary step in the spatial scale analysis, Sianturi et al. (2018) and the Ministry of Public Works and Housing clustered the four regencies in the northern

area, namely, Bekasi Regency, Karawang Regency, Subang Regency, and Indramayu Regency, as an agricultural area served by the Jatiluhur Dam, referred as dam-irrigated regencies in this study. On the other hand, the other regencies are irrigated by local water resources, like rivers or wells, referred to as local water resource-irrigated regencies in this study. The boundaries of these regions can be seen in Fig. 6. Based on this classification, the spatial assessment was carried out by grouping each grid into those two categories.

4.2 Spatial scale analysis

Crop yield estimation model on the grid scale was generated using multilinear regression analysis in Python to select the most significant NDVI images. Non-significant variables with large *p*-values were eliminated using stepwise elimination, as recommended by Freund and Littell (1991). The detrended crop yield was the dependent

Fig. 6 Map of dam-irrigated and local water resource-irrigated area in West Java



variable, and it was calculated using monthly crop production data during the dry cropping season. Meanwhile, the smoothed NDVI values during the dry cropping period (NDVI-7 until NDVI-18, as detailed in Table 2) were the independent variables. Through stepwise multilinear regression analysis, the crop yield estimation model was obtained following this equation:

$$\text{Crop Yield (Ton/Ha)} = 9.94 - 29.33 \text{ NDVI9} + 42.61 \text{ NDVI10} - 24.75 \text{ NDVI11} + 32.68 \text{ NDVI15} - 57.33 \text{ NDVI16} + 30.28 \text{ NDVI17\#} \quad (4)$$

Figure 7 displays the annual average NDVI value across the entire agricultural region of the study area. The green box indicated the wet cropping season while the red box indicated the dry cropping season as the focus of this study. The yellow-cross marker within the red box represented the significant NDVI images based on the result of crop yield estimation model. Based on this outcome, the significant NDVI images were predominantly observed during the peak and the end of the dry cropping season or around the harvesting period. The validation of the model revealed an *r*-value of approximately 0.83 when applied to the training dataset and approximately 0.71 when applied to the test dataset, as shown in Fig. 8.

Then, the crop yield estimation model was applied to generate the crop yield data from 2001 to 2020 in the agriculture area. And for the correlation analysis, the detrended method using LOWESS was applied to obtain the detrended crop yield dataset from 2001 to 2020 on each grid as an indicator of agricultural drought risk. As previously mentioned on Section 3.3.3, the detrended crop yield value lower than one can represent crop yield loss. Appendix 3 and Appendix 4 show the results of crop yield estimation and detrended crop yield, respectively. Figure 9 shows the result of Pearson correlation analysis between drought events indicated by the SPI and detrended crop yield with *p*-value < 0.05. The positive correlation resulted from this analysis indicated that crop yield loss more likely occurred during the drought event, indicated by low SPI. The correlation values were varied from around 0 to larger than 0.7, which can indicate the strength of drought conditions that affected crop yield. The low significant *r*-value was caused by the low number of data points as the input for correlation analysis, meaning that drought events occurred relatively low in some grids over the 20-year period.

Figure 10 shows the *r*-value distribution in each grid during the most severe drought year. The vertical axis

Fig. 7 Significant NDVI images for crop yield model on the grid scale

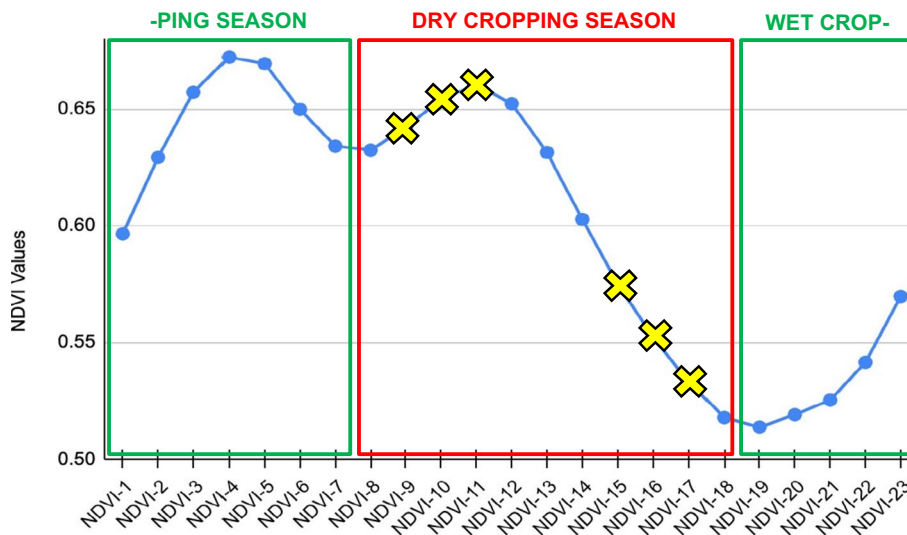


Fig. 8 Crop yield model validation on the grid scale

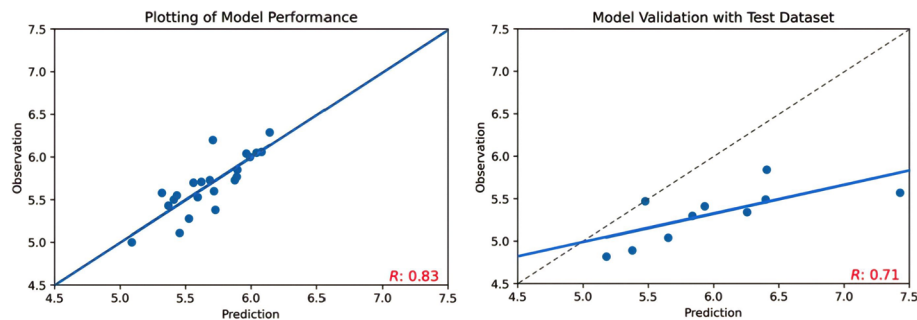


Fig. 9 Map of the correlation between detrended crop yield and SPI-3 on the grid scale.

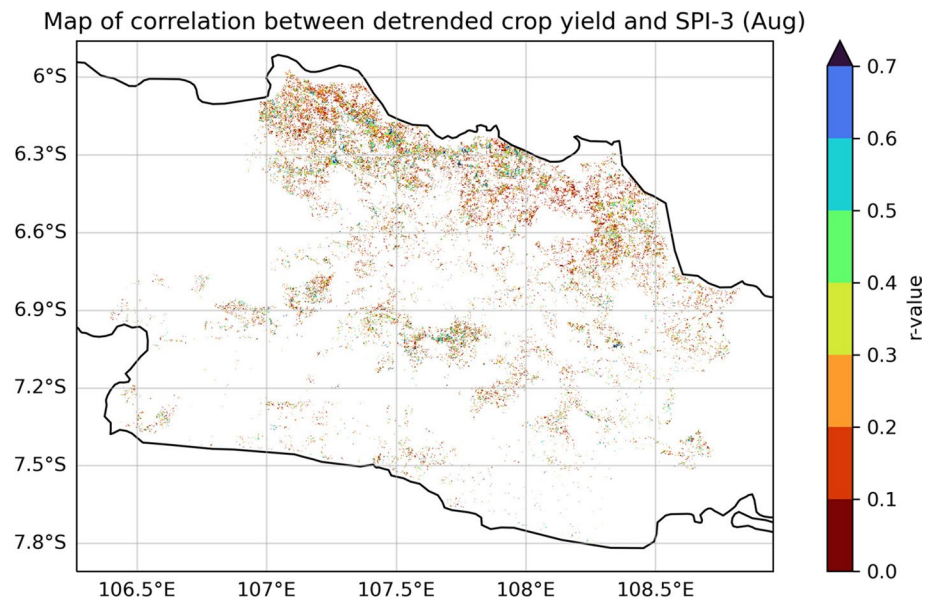
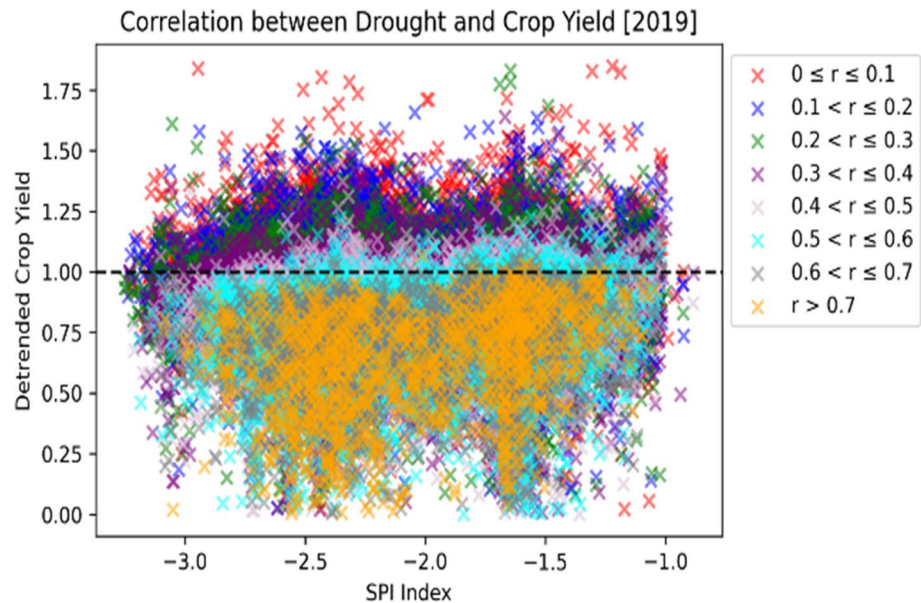


Fig. 10 Data characteristics of R -value



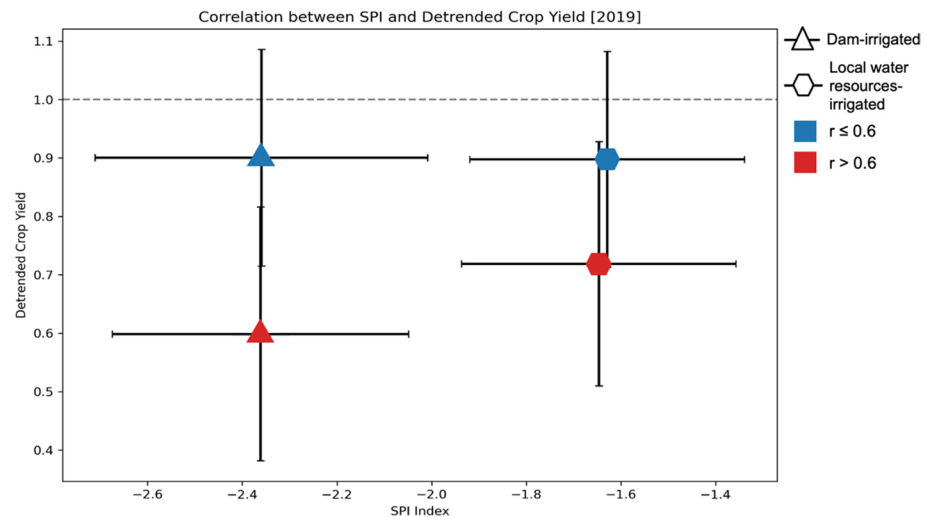
represents the crop yield and the horizontal axis represents the drought condition. The results indicate that the region with an r -value > 0.6 , depicted by the grey and orange color, is mostly located below the average detrended crop yield lane, signifying their vulnerability to drought, as proven by a reduction in crop yield across almost all grids.

The study further analyzed the data by categorizing the grids according to the irrigation system, as shown in Fig. 6. The results of the correlation analysis between the SPI and detrended crop yield are presented in Fig. 11, where the triangle-shaped marker indicates the irrigated area, and the hexagonal-shaped marker indicates the local water resource-irrigated area. The blue color indicates

the area with an r -value less than 0.6; meanwhile, the red color indicated the r -value larger than 0.6. The vertical line in Fig. 11 represents the error bar for detrended crop yield, indicating the variability of agricultural drought risk, which could result in crop yield gain (if larger than 1) or crop yield loss (if less than 1) among all grids. On the other hand, the horizontal line represents the error bar for the SPI, indicating the different degrees of hazard among all grids.

The analysis showed that the irrigated area was located on the left side or in regions of more severe drought conditions. This result indicates that the purpose of the irrigation system to supply water in the area that might be hit by drought was

Fig. 11 Correlation between SPI and detrended crop yield based on the existence of irrigation system

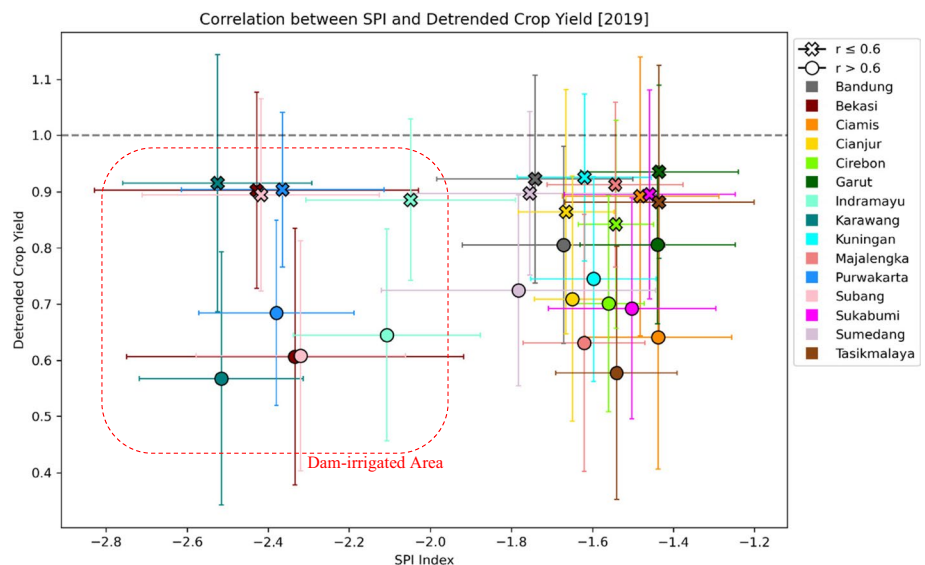


achieved. However, in the regions with an r -value larger than 0.6 (denoted by the red color), which were more vulnerable to drought, higher drought magnitude resulted in a greater crop yield loss, indicating that the drought hazard was one of the key drivers of yield loss. In contrast, there was no observed difference in crop yield loss in regions with an r -value less than 0.6 (denoted by the blue color) suggesting that the existence of an irrigation system helped to resist the impact of agricultural drought, resulting in the same crop yield loss as the local water resource-irrigated area, even when affected by more severe drought. Nevertheless, this hazard assessment alone is insufficient to explain the varied responses of wet farming crops during the dry cropping season to agricultural drought, both in the dam-irrigated area and local water resource-irrigated area; thus, further study is necessary. Some of the studies, for example, focused on the vulnerability assessment to explore the sensitivity of

agricultural drought risk to the possible key driver factors on a specific study location (Wilhemi et al. 2002; Jianjun Wu et al. 2011; Di Wu et al. 2013; Murthy et al. 2015; Hao Wu et al. 2017)

The subsequent analysis focused on the correlation between SPI and detrended crop yield at the city scale, in which the result can be seen in Fig. 12. Each color in the figure corresponds to a different city, while the vertical and horizontal axes, as well as the error bar, have the same meaning as in the previous analysis. In this analysis, the grid-scale data was aggregated into a city scale. The findings indicate that in the region with an r -value less than 0.6, or indicated by x-shaped marker, the dry condition is not the primary factor driving crop yield loss. This was proven by the value of the detrended crop remaining consistent despite the SPI ranging from -1.2 until -2.8 . Conversely, in the region with an r -value larger than 0.6 (indicated by an o-shaped

Fig. 12 Correlation between SPI and detrended crop yield on city-scale aggregation



marker), which is strongly associated with drought, the crop yield loss varied but was generally more severe than in other regions. These results also emphasize the importance of assessing agricultural drought at a finer resolution, as wet farming crop responses during the dry cropping season can vary even within the same city.

A notable observation in this figure is the location of the four cities served by the Jatiluhur Dam (refer to Fig. 6), along with the Purwakarta Regency, where the dam is situated (marked within the red-dashed square), located on the far left of the diagram, indicating that those regions are among the most severely affected by drought. Nevertheless, while the irrigation system was constructed to mitigate crop yield loss, the effectiveness of those systems varied in different agricultural areas, with some regions experiencing less crop yield loss than others. This finding also amplifies the previous statement that the significant role played by other factors in determining the impact of drought on crop yield loss that needs further investigation, while for Hendrawan et al. (2023) who assessed the possible key factors of crop yield sensitivity to drought on global scale, the local assessment is also needed to understand the local factors especially in the fragmented agricultural areas.

5 Summary and conclusion

The objective of this study was to address the gap in agricultural drought assessment for the wet farming crops. From this study, it was revealed that SPI-3 during August is the most suitable timescale for agricultural drought assessment on wet farming crops in the target area. This finding is consistent with the result of previous study by Umran in 1999, which stated that SPI-3 is sensitive to the reduction in soil moisture that affects crop growth, and with a study by Ji and Peters 2002, which stated that vegetation has a time-lagged response to precipitation, with the impact of water deficits being cumulative. It is noteworthy that the crop calendar and precipitation distribution vary across regions or countries, which can have a significant impact on the result. Furthermore, the difference in agreement among the regions between observed precipitation data and satellite-based precipitation data shown in Fig. 3 might also contribute to the uncertainty of this finding. Nonetheless, this limitation is beyond the scope of this study.

The spatial assessment on the grid scale revealed that there is a negative correlation between the SPI and detrended crop yield, indicating that crop yield loss is associated with dry conditions. This finding emphasizes the importance of conducting agricultural drought risk assessment on finer resolution. The thresholding of the r -value at

0.6 suggests that in the regions with an r -value larger than 0.6, dry conditions are the primary driver of crop yield loss during the dry cropping season, even in the presence of an irrigation system. Those regions also can be said as the area which is more vulnerable to drought. Conversely, in the region with an r -value less than 0.6, dry conditions are not the primary driver of crop yield loss, and the existing irrigation system was able to resist the drought's impact on crop yield loss.

This study has revealed the potential influence of additional factors in determining the impact of drought on crop yield loss, which highlights the necessity of conducting further research to explore the agricultural drought vulnerability on wet farming crops. Future investigations should scrutinize the impact of multiple factors, such as water accessibility, socioeconomic condition, and other climate parameters, to provide a more comprehensive understanding of the impact of drought on agriculture areas at a finer resolution.

6 Supplementary information

Supplementary Information The online version contains supplementary material available at <https://doi.org/10.1007/s00704-023-04461-w>.

Acknowledgements This work was supported by the International Joint Graduate Program in Resilience and Safety Studies (GP-RSS) and Green Goals Initiative, Tohoku University. We would like to express our gratitude to Dr. Rima from the Meteorology, Climatology, and Geophysical Agency of Indonesia and Dr. Sudarmadi, Dr. Iskandar, and Dr. Yayan from the Agricultural Agency of West Java, who helped us with the required dataset. We also thank anonymous reviewers for their constructive comments and suggestions, which led to substantial improvements in our manuscript.

Author contribution All the authors contributed to conceptualizing, designing, and discussing the study and result. Daisuke Komori and Vempi Satriya Adi Hendrawan supervised the findings of this work, provided critical feedback, and helped shape the research. Amalia Nafisah Rahmani Irawan gathered data; Amalia Nafisah Rahmani Irawan did the programming code with help from Vempi Satriya Adi Hendrawan; the initial draft of the paper was prepared by Amalia Nafisah Rahmani Irawan and reviewed by Vempi Satriya Adi Hendrawan; the article was repeatedly revised to generate the final version by Daisuke Komori.

Funding This work was supported by JST SPRING, Grant Number JPMJSP2114.

Data availability The precipitation and NDVI data are available in the public domain at the links provided in the texts. The agricultural statistical data is available from the corresponding author on reasonable request.

Code availability The codes used for the processing of data can be provided on request to the corresponding author.

Declarations

Ethics approval Not applicable.

Consent to participate The authors declare that they have consent to participate in this paper.

Consent for publication The authors declare that they have consent to publish in this journal.

Competing interests The authors declare no competing interests.

Open Access This article is licensed under a Creative Commons Attribution 4.0 International License, which permits use, sharing, adaptation, distribution and reproduction in any medium or format, as long as you give appropriate credit to the original author(s) and the source, provide a link to the Creative Commons licence, and indicate if changes were made. The images or other third party material in this article are included in the article's Creative Commons licence, unless indicated otherwise in a credit line to the material. If material is not included in the article's Creative Commons licence and your intended use is not permitted by statutory regulation or exceeds the permitted use, you will need to obtain permission directly from the copyright holder. To view a copy of this licence, visit <http://creativecommons.org/licenses/by/4.0/>.

References

- Angelidis P et al (2012) Computation of drought index SPI with alternative distribution functions. *Water Resour Manag* 26(9):2453–2473
- Balaghi R et al (2008) Empirical regression models using NDVI, rainfall and temperature data for the early prediction of wheat grain yields in Morocco. *Int J Appl Earth Obs Geoinformation* 10(4):438–452
- Blain GC (2011) Standardized precipitation index based on Pearson type III distribution. *Revista Brasileira de Meteorologia* 26:167–180
- Chen J et al (2004) A simple method for reconstructing a high-quality NDVI time-series data set based on the Savitzky-Golay filter. *Remote Sens Environ* 91(3–4):332–344
- Dai M et al (2020) Assessing agricultural drought risk and its dynamic evolution characteristics. *Agric Water Manag* 231:106003
- D'Arrigo Rosanne, Wilson Rob (2008) El Nino and Indian Ocean influences on Indonesian drought: implications for forecasting rainfall and crop productivity. *Int J Climatol: J Royal Meteorol Soc* 28(5):611–616
- Didan, K. (2015). *MOD13Q1 MODIS/Terra vegetation indices 16-day L3 global 250m SIN grid V006*. NASA EOSDIS Land Processes DAAC. Accessed 2022-04-30 from <https://doi.org/10.5067/MODIS/MOD13Q1.006>
- Dutta D, Arnab K, Patel NR (2013) Predicting agricultural drought in eastern Rajasthan of India using NDVI and standardized precipitation index. *Geocarto Int* 28(3):192–209
- FAO (2015) The impact of disasters on agriculture and food security, vol. 77, FAO, Rome
- FAO (2003) WTO agreement on agriculture: the implementation experience – developing country case studies, FAO, Rome
- Freund RJ, Littell RC (1991) SAS system for regression, 2nd edn. SAS Institute Inc., Cary, NC
- Geng G et al (2016) Agricultural drought hazard analysis during 1980–2008: a global perspective. *Int J Climatol* 36(1):389–399
- Guttman NB (1999) Accepting the standardized precipitation index: a calculation algorithm 1. *JAWRA J Am Water Resour Assoc* 35(2):311–322
- Hendrawan VSA et al (2022) A global-scale relationship between crop yield anomaly and multiscale drought index based on multiple precipitation data. *Environ Res Lett* 17(1):014037
- Hendrawan VS, Adi DK, Kim W (2023) Possible factors determining global-scale patterns of crop yield sensitivity to drought. *Plos one* 18(2):e0281287
- Hirabayashi Y et al (2008) Global projections of changing risks of floods and droughts in a changing climate. *Hydrol Sci J* 53(4):754–772
- Huang J et al (2014) Analysis of NDVI data for crop identification and yield estimation. *IEEE J Sel Top Appl Earth Obs Remote Sens* 7(11):4374–4384
- Iglesias A, Quiroga S (2007) Measuring the risk of climate variability to cereal production at five sites in Spain. *Clim Res* 34(1):47–57
- Ionita Monica, Nagavciuc Viorica (2021) Changes in drought features at the European level over the last 120 years. *Nat Hazards Earth Syst Sci* 21(5):1685–1701
- IPCC, 2018: Summary for policymakers. In: *Global warming of 1.5°C. An IPCC Special Report on the impacts of global warming of 1.5°C above pre-industrial levels and related global greenhouse gas emission pathways, in the context of strengthening the global response to the threat of climate change, sustainable development, and efforts to eradicate poverty* [Masson-Delmotte, V., P. Zhai, H.-O. Pörtner, D. Roberts, J. Skea, P.R. Shukla, A. Pirani, W. Moufouma-Okia, C. Péan, R. Pidcock, S. Connors, J.B.R. Matthews, Y. Chen, X. Zhou, M.I. Gomis, E. Lonnoy, T. Maycock, M. Tignor, and T. Waterfield (eds.)]. In Press
- Ji Lei, Peters Albert J (2003) Assessing vegetation response to drought in the northern Great Plains using vegetation and drought indices. *Remote Sens Environ* 87(1):85–98
- Karavitis CA et al (2011) Application of the standardized precipitation index (SPI) in Greece. *Water* 3(3):787–805
- Kumar U et al (2021) Use of meteorological data for identification of agricultural drought in Kumaon region of Uttarakhand. *J Earth Syst Sci* 130(3):121
- Legesse GIZACHEW (2010) Agricultural drought assessment using remote sensing and GIS techniques. Addis Ababa University, Department of Earth Science
- Lehner B et al (2006) Estimating the impact of global change on flood and drought risks in Europe: a continental, integrated analysis. *Clim Change* 75(3):273–299
- Lugo AE, Brown S (1992) Tropical forests as sinks of atmospheric carbon. *Forest Ecol Manag* 54(1–4):239–255
- Maryati S, Humaira ANS, Pratiwi F. “Spatial pattern of agricultural land conversion in West Java Province.” *IOP Conference Series: Earth and Environ Sci*. Vol. 131. No. 1. IOP Publishing, 2018.
- Maselli F, Rembold F (2001) Analysis of GAC NDVI data for crop-land identification and yield forecasting in Mediterranean African countries. *Photogramm Eng Remote Sens* 67:593–602
- McKee, Thomas B., Nolan J. Doesken, and John Kleist. “The relationship of drought frequency and duration to time scales.” *Proceedings of the 8th Conference on Applied Climatology*. Vol. 17. No. 22. 1993.
- Mkhabela MS, Mkhabela MS, Mashinini NN (2005) Early maize yield forecasting in the four agro-ecological regions of Swaziland using NDVI data derived from NOAA's-AVHRR. *Agric Forest Meteorol* 129(1–2):1–9
- Moccia, Benedetta, et al. “SPI-based drought classification in Italy: influence of different probability distribution functions.” *Water* 14.22 (2022): 3668.

- Mourtzinis S, Juan IRE, Shawn PC, Patricio G (2017) From grid to field: assessing quality of gridded weather data for agricultural applications. *Eur J Agron* 82:163–172
- Murthy CS, Laxman B (2015) Sesa Sai MVR “Geospatial analysis of agricultural drought vulnerability using a composite index based on exposure, sensitivity and adaptive capacity.” *Int J Dis Risk Reduction* 12:163–171
- Naresh Kumar M, Murthy CS, Sesa Sai MVR, Roy PS (2012) Spatiotemporal analysis of meteorological drought variability in the Indian region using standardized precipitation index. *Meteorol Appl* 19(2):256–264
- Pan Z, Jingfeng H, Qingbo Z, Limin W, Yongxiang C, Hankui Z, George AB, Jing Y, Jianhong L (2015) Mapping crop phenology using NDVI time-series derived from HJ-1 A/B data. *Int J Appl Earth Obs Geoinformation* 34:188–197
- Pieper, Patrick, André Düsterhus, and Johanna Baehr. “Global and regional performances of SPI candidate distribution functions in observations and simulations.” *EGU General Assembly Conference Abstracts*. 2020.
- Pramudya, Y., and T. Onishi. “Assessment of the standardized precipitation index (SPI) in Tegal City, Central Java, Indonesia.” *IOP conference series: earth and environmental science*. Vol. 129. No. 1. IOP Publishing, 2018.
- Ribeiro AFS, Pires CAL (2016) Seasonal drought predictability in Portugal using statistical–dynamical techniques. *Phys Chem Earth, Parts A/B/C* 94:155–166
- Salati E, Lovejoy TE, Vose PB (1983) Precipitation and water recycling in tropical rain forests with special reference to the amazon basin. *Environmentalist* 3(1):67–72
- Shah Ravi, Bharadiya Nitin, Manekar Vivek (2015) Drought index computation using standardized precipitation index (SPI) method for Surat District, Gujarat. *Aquatic Procedia* 4:1243–1249
- Shiau Jenq-Tzong (2020) Effects of gamma-distribution variations on SPI-based stationary and nonstationary drought analyses. *Water Resour Manag* 34(6):2081–2095
- Sianturi R, Jetten VG, Sartohadi Junun (2018) Mapping cropping patterns in irrigated rice fields in West Java: towards mapping vulnerability to flooding using time-series MODIS imageries. *Int J Appl Earth Obs Geoinformation* 66:1–13
- Son NT et al (2014) A comparative analysis of multitemporal MODIS EVI and NDVI data for large-scale rice yield estimation. *Agric Forest Meteorol* 197:52–64
- Stage JH, Tallaksen LM, Gudmundsson L, Van Loon AF, Stahl K (2015) Candidate distributions for climatological drought indices (SPI and SPEI). *Int J Climatol* 35(13):4027–4040
- Surmaini, Elza, and Akhmad Faqih. “Kejadian iklim ekstrem dan dampaknya terhadap pertanian tanaman pangan di Indonesia.” *Jurnal Sumberdaya Lahan* 10.2 (2016). (in Bahasa Indonesia)
- Tashima T et al (2020) Precipitation extremes monitoring using the near-real-time GSMaP product. *IEEE J Sel Top Appl Earth Obs Remote Sens* 13:5640–5651
- Trenberth, Kevin E (2005) The impact of climate change and variability on heavy precipitation, floods, and droughts. *Encycl hydrol sci* 17
- Umran Komuscu, Ali (1999) Using the SPI to analyze spatial and temporal patterns of drought in Turkey. *Drought Network News* (1994–2001):49
- Vicente-Serrano SM, López-Moreno J (2005) Hydrological response to different time scales of climatological drought: an evaluation of the Standardized Precipitation Index in a mountainous Mediterranean basin. *Hydrol Earth Syst Sci* 9(5):523–533
- Wang H, Chen Y, Pan Y, Chen Z, Ren Z (2019) Assessment of candidate distributions for SPI/SPEI and sensitivity of drought to climatic variables in China. *Int J Climatol* 39(11):4392–4412
- Wilhelmi Olga V, Wilhite Donald A (2002) Assessing vulnerability to agricultural drought: a Nebraska case study. *Nat Hazards* 25:37–58
- Wilhite Donald A, Glantz Michael H (1985) Understanding: the drought phenomenon: the role of definitions. *Water Int* 10(3):111–120
- WMO (2012) Standardized Precipitation Index user guide. WMO-No. 1090, World Meteorological Organization, Geneva
- Wu J, He B, Lü A, Zhou L, Liu M, Zhao L, Wu J et al (2011) Quantitative assessment and spatial characteristics analysis of agricultural drought vulnerability in China. *Nat Hazards* 56:785–801
- Wu D, Yan DH, Yang GY, Wang XG, Xiao WH, Zhang HT (2013) Assessment on agricultural drought vulnerability in the Yellow River basin based on a fuzzy clustering iterative model. *Nat hazards* 67:919–936
- Wu H, Qian H, Chen J, Huo C (2017) Assessment of agricultural drought vulnerability in the Guanzhong Plain, China. *Water Resour Manag* 31:1557–1574
- Xue J and Su B (2017) Significant remote sensing vegetation indices: a review of developments and applications. *Journal of sensors* 2017
- Ying Zhang and Zhanling Li (2020) Uncertainty analysis of standardized precipitation index due to the effects of probability distributions and parameter errors. *Front in Earth Sci* 8:76
- Zhang Y, Li Z (2020) Uncertainty analysis of standardized precipitation index due to the effects of probability distributions and parameter errors. *Front Earth Sci* 8:76

Publisher's note Springer Nature remains neutral with regard to jurisdictional claims in published maps and institutional affiliations.